URSI AP-RASC, Sydney, Australia, 17 – 22 August 2025

Analysis of Bit Stream Combinations and Tag Encoding in Chipless RFID Tag

Hafsa Anam* [(1)], Syed Muzahir Abbas [(1)], Iain B. Collings [(1)], and Subhas C. Mukhopadhyay [(1)]
(1) School of Engineering, Macquarie University, 2109 NSW Australia.

Abstract

This paper investigates various bit stream combinations, focusing on their application in encoding and data representation in chipless RFID (radio frequency identification) tags. An 18-bit tag is used for threshold determination to read the RCS (radar cross-section) bits. The dual-sided tag's response resonates at 4.5GHz-11.5GHz frequency band. Once we read the UID (unique identification) code at VNA (vector network analyzer), a threshold is defined that can read possible dips as 1's below -33dBsm, and possible peaks as 0's above -29dBsm. The response between these two threshold points is very minor and considered as noise/attenuation. Additionally, we analyze the role of threshold values in determining the accuracy and precision of data bit readings, particularly in environments where signal degradation may occur. Through experimentation and simulation, this study identifies optimal encoding strategies and threshold settings to enhance the efficiency of chipless RFID tags, contributing to the advancement of this technology for real-world applications in supply chain management, asset tracking, and beyond.

1. Introduction

A standard passive chipless RFID system typically includes a transponder, often referred to as a tag, a reader system that may consist of multiple components based on requirements and the tag, along with transmitter and receiver antennas, and a server or host system [1].
Traditional RFID systems rely on microchips to store and transmit data, but the emerging field of chipless RFID offers a promising alternative by eliminating the need for these chips. Chipless RFID tags encode data in the form of electromagnetic signals, typically through resonant structures or frequency-dependent characteristics, making them cost-effective and highly scalable. This innovation is particularly attractive for applications in asset tracking, inventory management, and supply chain logistics, where low-cost, disposable tags are essential [2].
Intelligent tracking/management process has four stages: a). digital signal captures the data, b). data is analyzed, c). Statistical information is captured, d). output is mapped as real time feedback [2]. So, the overall process involves collection of information/data, its manipulation/detection, and transmission to reader at server, leading to an efficient system. The unprecedented aspects of passive techniques make the system cost efficient, energy sufficient and uncomplicated process, with overall increment in efficiency. A basic chipless RFID system is shown in Fig. 1.
In 2023, Abdullah et.al., presented a tactile passive switch, which operates via physical motion [3]. The switch is an RF tag, embedded with tactile-sensitive material. The researcher has designed the tag with a sensing resonator and two ID resonators for identification. The switch operation is touch-controlled and is measured as frequency fluctuation over the sensing resonator response. It has now been proposed that for increased data capacity, hybrid encoding technique plays an amazing role [4]. Herein, the encoding approach increment data states from 32 to 243, with tremendous data capacity. More recent research shows the evidence of passive RFID technology application areas are expanding. Ranging from temperature and crack sensor [5], water level detector [6], water leakage detection [7], soil moisture sensor [8], fluid pathways blockage detection sensor [9], corrosion sensor [10], to keypad sensor [11], and wearable sensor for skin [12-14] are diverse targeted areas of researchers in past few years. Research has been done in design and sensing domains; however, challenges remain in optimizing data encoding methods and ensuring reliable data retrieval, particularly in environments prone to signal interference. This paper delves into the various encoding techniques and threshold parameters critical for the accurate reading of chipless RFID tags, aiming to improve the robustness and efficiency of the system for practical use.
This paper presents an approach towards threshold definition while reading RCS response of chipless RFID tags. The considerable dips are read as '1' bit, the readable peaks are encoded as '0' bit, whereas the notches that appear out of threshold levels are considered as noise/attenuation. The paper is structured: Section 2 explains the Tag and its response, Section 3 illustrates the RCS response reading and threshold analysis, Section 4 explains the measured and simulated response with reliability analysis. The conclusion is drawn in Section 5.

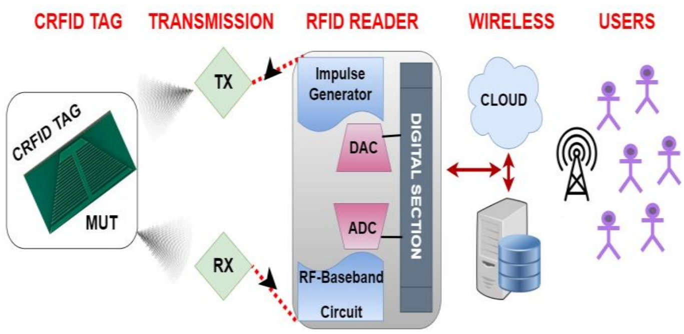

Figure 1. Basic chipless RFID System.

2. Chipless RFID Tag

An 18-bit chipless RFID tag has been opted from previous work for data encoding and reading [15]. The battery-free tag has 18 slots, that resonate at 18 unique frequencies. Fig. 2 shows RCS response of chipless RFID tag with tag design. 4.5GHz-11.5GHz is the frequency band of designed tag. A chipless RFID tag is essentially a metal component lacking embedded intelligence for communication with the reader. As a result, chipless RFID requires significant research and approaches towards better and reliable performance with innovative design approaches.

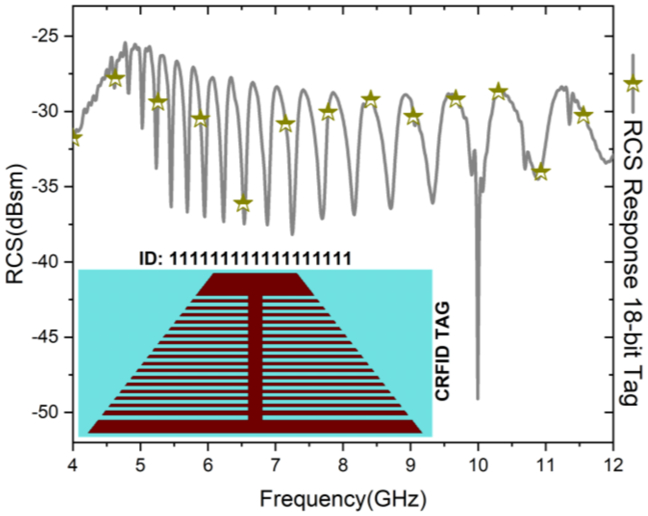

Figure 2. RCS Response of 18-bit Chipless Tag.

Fig. 3 shows current distribution at three frequencies 4Ghz, 8.5GHz and 12GHz. The response of tag is captured in the radio waves and re-transmitted backwards to the reader via receiver antenna. The reader selection varies depending upon the type of tag, operational frequency, application type and many other factors specific to a unique tag. But a generic reader unit holds antennas for transmission and reception of signals, analog to digital (ADC) and digital to analog converter (DAC), impulse generator, an RF baseband processing circuit, and digital monitoring section. Data is captured as binary combination of “1 and 0”, referred to as “unique identification code” (UID). In RCS response, all dips are marked as ‘1’ bit and peaks are referred to as ‘0’.

While designing the tag, a unique resonance frequency at which a particular slot resonates is acquired depending upon the length of slot. The relation between slot length and RCS response, and the effect of slot width on the output response is shown in Fig. 4. It can be clearly seen that with increment in slot length, the resonance frequency is decreasing linearly, also RCS magnitude shifts towards lower values. Regarding slot width, there is no variation in frequency, whereas mild fluctuation in RCS values is observed.

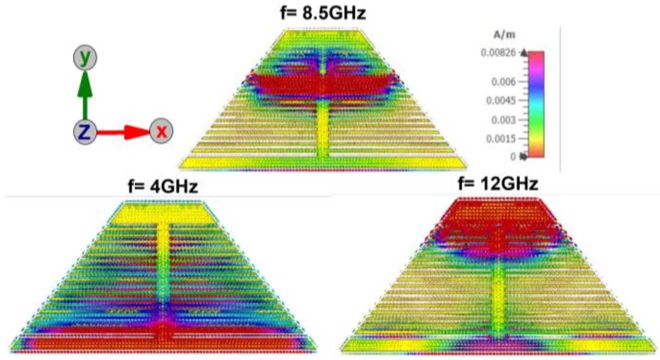

Figure 3. Surface Current Distribution of CRFID Tag.

To acquire a desired frequency band, these parameters play a vital role. Each resonator designed in the tag is particular towards resonance frequency (f_r). The largest slot corresponds to smallest frequency (MSB) whereas, (LSB) at largest frequency is response from smallest resonator. Each resonator has unique resonance frequency, given by (5) [15]

$$f_r = \frac{c}{2L}\sqrt{2/(\varepsilon_r + 1)} \quad (1)$$

Where, $'L'$ is length of a particular slot in tag and $'\varepsilon_r'$ is dielectric permittivity, and $'c'$ is speed of light.

As the slot length varies, the resonance frequency changes. The response graphically illustrates the relation between; (a) slot length vs. and resonance frequency and RCS (b) Slot width vs. resonance frequency and RCS. In first, we can visualize that with increasing slot length, the frequency and RCS are decreasing. RCS is stable after 0.8mm slot length. Whereas second graph shows that slot width does not affect frequency much, it is effecting RCS of signal. The major direct relation from response is the inverse relation between slot length and resonance frequency.

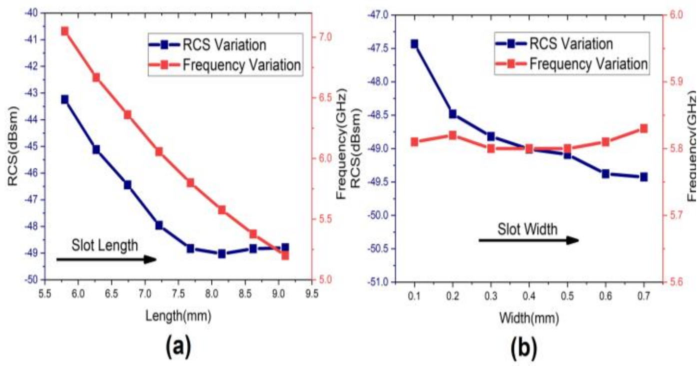

Figure 4. Parametric Analysis of Designed Tag.

3. Results And Analysis

The RCS response of chipless tag is utilized for reading RCS via Vector network analyzer (VNA). Five fabricated samples have been tested for the measured results. Fig. 5

shows the reliability response of proposed fabricated chipless RF tag. Performance analysis of the tag is reliable and shows great accordance compared with actual test results. The response illustrates the reliability curve of proposed tag, which gives a (+0.035) and (-0.035) tolerance in frequency values, whereas (+0.025) and (-0.025) are the fluctuation in RCS magnitude. This range is quite reliable for detection of dips resonating at unique frequency.

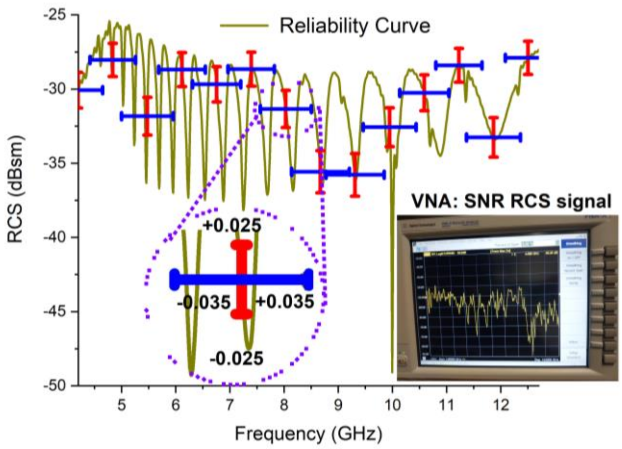

Figure 5. Reliability Curves of the Proposed Tag.

For readers, the response needs to have a threshold level for detection of 1's and 0's. In general, a tag should be able to identify 2^n number of unique objects. For 18-bit tag, 218 possible combinations can be acquired. To acquire these varying sets of binary data, we need to alternate the 1's in the data bits with 0's. This concept is referred to as 'shortening of tag'. A single slot in the designed tag generates 1-dip in RCS response, this dip is labelled as '1-bit' in binary data. To acquire '0' in the combination, we invert the process, i.e., fill the slot with metal. This shortening of slot process embeds and replaces a '0' in the data and dips in response inverts to the peak.

Fig. 6 (a, b, c) shows various possible combinations. The first figure shows two possible combinations, all 0's and all 1's yielding '000000000000000000' and '111111111111111111' bit stream. Alternate bits for 18-bit tag with binary code '101010101010101010' are shown in second graph. Whereas the third graph shows random data stream '010101011010101101'.

First, we defined RCS levels at two points i) -29dBsm ii) -33dBsm. The spread of RCS values can vary from tag to tag, depending upon tag's size, structure, design, and slots. These threshold values separate the RCS values into two distinct levels, via a numerical value that acts as a cutoff point between "low" and "high" RCS responses. In this case, -29dBsm and -33dBsm are numerical cut-off values. If the tag response has noise and attenuation, it can be hard to define cut-off values from graph. Then, we can take mean of values for defining a threshold level.

In future, work needs to be considered for adaptive environments, where in some cases, the threshold may need to be adaptive. You could employ adaptive thresholding where the system continuously adjusts the threshold based on changing conditions such as tag position, orientation, or interference.

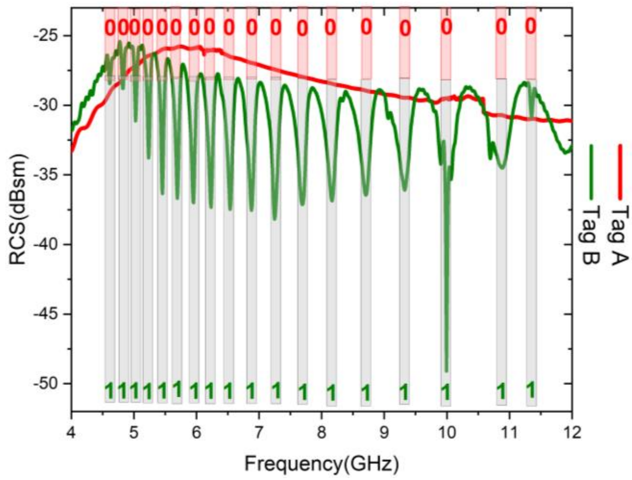

Figure 6(a). Multi-ID Combination-All 1's and 0's.

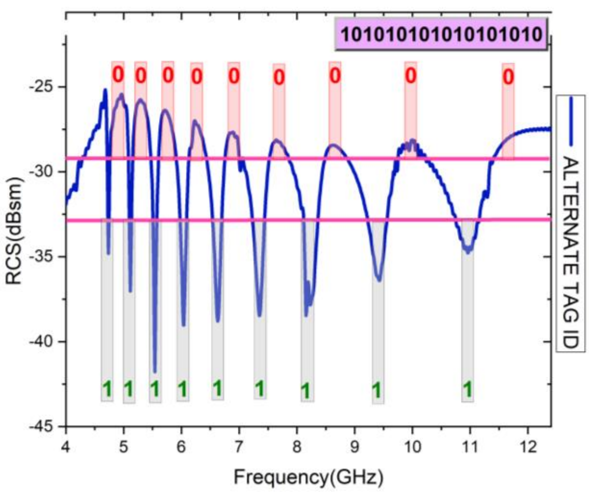

Figure 6(b). Multi-ID Combination-Alternate bits.

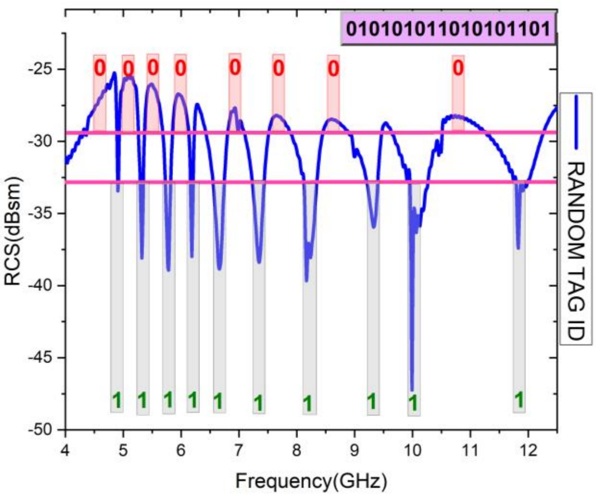

Figure 6(c). Multi-ID Combination-Random ID.

4. Conclusion

This paper provides a comprehensive analysis of bit stream combinations and their impact on encoding and data representation in chipless RFID tags. By focusing on threshold determination and examining the response of an 18-bit dual-sided tag in the 4.5GHz-11.5GHz frequency band, the study successfully establishes a framework for reading UID codes. The identification of optimal threshold values, distinguishing between dips as 1's and peaks as 0's, highlights the importance of precise threshold settings in mitigating signal noise and ensuring accurate data readings. Experimental and simulation results further demonstrate the potential for enhanced efficiency in chipless RFID tags, suggesting improvements for real-world applications in areas like supply chain management and asset tracking. In the future, it will be important to account for adaptive environments, where the threshold may need to be adjusted dynamically. Adaptive thresholding can be implemented, allowing the system to continuously modify the threshold in response to varying conditions.

5. Acknowledgements

We would like to express our gratitude to Macquarie University for their support and research assistance.

References

[1] N. C. Karmakar, E. Md. Amin and J. K. Saha, "Case Studies," in *Chipless RFID Sensors*, Wiley, 2016, pp.225-242, doi: 10. 1002/ 9781119078104.

[2] S. Xu, F. Xiao, N. Si, L. Sun, W. Wu and V. H. C. de Albuquerque, "GQM: Autonomous goods quantity monitoring in IIoT based on battery-free RFID," in Mechanical Systems and Signal Processing, 2020, vol. 136, no. 106411, pp. 0888-3270, 2020, doi: 10.1016/j.ymssp.2019.106411.

[3] A. S. Almansouri, "Tactile Light Switch Using Chipless RFID," in *IEEE Sensors Letters*, vol. 7, no. 9, pp. 1-4, Sept. 2023, Art no. 2502504, doi: 10.1109/LSENS.2023.3301829.

[4] A. Lalbakhsh *et al.*, "Hybrid Encoding Method for Radio Frequency Identification in the Internet of Things Systems," in *IEEE Access*, vol. 11, pp. 122554-122565, 2023, doi: 10.1109/ACCESS.2023.3326719.

[5] N. Javed, M. A. Azam and Y. Amin, "Chipless RFID Multisensor for Temperature Sensing and Crack Monitoring in an IoT Environment," in *IEEE Sensors Letters*, vol. 5, no. 6, pp. 1-4, June 2021, Art no. 6001404, doi: 10.1109/LSENS.2021.3083218.

[6] A. Guillet, A. Vena, E. Perret and S. Tedjini, "Design of a chipless RFID sensor for water level detection," *2012 15 International Symposium on Antenna Technology and Applied Electromagnetics*, Toulouse, France, 2012, pp. 1-4, doi: 10.1109/ANTEM.2012.6262372.

[7] W. Weiming, W. Jian and T. Kun, "Development of a Chipless RFID Water Leakage Detecting Sensor Using Defected Ground Structure," *2022 International Applied Computational Electromagnetics Society Symposium (ACES-China)*, Xuzhou, China, 2022, pp. 1-2, doi: 10.1109/ACES-China56081.2022.10064942.

[8] X. Qi, Y. Fan and X. Liu, "Depolarized L-Shaped Chipless RFID Sensor Tag for Soil Moisture Monitoring," *2023 International Conference on Microwave and Millimeter Wave Technology (ICMMT)*, Qingdao, China, 2023, pp. 1-3, doi: 10.1109/ICMMT58241.2023.10276965.

[9] T. Athauda and N. Karmakar, "Chipless RFID sensor for blockage monitoring in fluid pathways," *2020 27th International Conference on Telecommunications (ICT)*, Bali, Indonesia, 2020, pp. 1-5, doi: 10.1109/ICT49546.2020.9239498.

[10] S. Deif and M. Daneshmand, "Multiresonant Chipless RFID Array System for Coating Defect Detection and Corrosion Prediction," in *IEEE Transactions on Industrial Electronics*, vol. 67, no. 10, pp. 8868-8877, Oct. 2020, doi: 10.1109/TIE.2019.2949520.

[11] U. A. Haider, M. Noman, H. Ullah, H. F. Abutarboush, Q. H. Abbasi and F. A. Tahir, "A Fully Passive Ten-Digit Numeric Keypad Sensor Using Chipless RFID Technology," in *IEEE Sensors Journal*, vol. 23, no. 3, pp. 2978-2987, 1 Feb.1, 2023, doi: 10.1109/JSEN.2022.3232154.

[12] S. K. Behera, "Chipless RFID Sensors for Wearable Applications: A Review," in *IEEE Sensors Journal*, vol. 22, no. 2, pp. 1105-1120, 15 Jan.15, 2022, doi: 10.1109/JSEN.2021.3126487.

[13] S. Dey, R. Bhattacharyya, S. E. Sarma and N. C. Karmakar, "A Novel "Smart Skin" Sensor for Chipless RFID-Based Structural Health Monitoring Applications," in *IEEE Internet of Things Journal*, vol. 8, no. 5, pp. 3955-3971, 1 March1, 2021, doi: 10.1109/JIOT.2020.3026729.

[14] J. G. D. Hester and M. M. Tentzeris, "Inkjet-printed Van-Atta reflectarray sensors: A new paradigm for long-range chipless low-cost ubiquitous Smart Skin sensors of the Internet of Things," 2016 IEEE MTT-S International Microwave Symposium (IMS), San Francisco, CA, USA, 2016, pp. 1-4, doi: 10.1109/MWSYM.2016.7540412.

[15] M. Baghelani, Z. Abbasi, M. Daneshmand and P. E. Light, "Noninvasive Microwave Sensor for Real-Time Continuous Dehydration Monitoring," in IEEE Sensors Journal, vol. 24, no. 7, pp. 9959-9969, 1 April1, 2024, doi: 10.1109/JSEN.2024.3362702.

[16] H. Anam, S. M. Abbas, S. Mukhopadhahy and I. Collings, "Dual Sided Data Dense 25-bit Chipless RFID Tag," 2023 IEEE International Symposium on Antennas and Propagation and USNC-URSI Radio Science Meeting (USNC-URSI), Portland, OR, USA, 2023, pp. 1487-1488, doi: 10.1109/USNC-URSI52151.2023.10237497.